

The binding site of the RNA-dependent protein kinase (PKR) on EBER1 RNA from Epstein–Barr virus

Momchilo Vuyisich, Richard J. Spanggord & Peter A. Beal*

University of Utah, Department of Chemistry, 315 S 1400 E, Room 2020, Salt Lake City, UT 84112, USA

Received February 22, 2002; revised May 23, 2002; accepted May 24, 2002

The RNA-dependent protein kinase (PKR) is an interferon-induced, RNA-activated enzyme that phosphorylates the eukaryotic initiation factor 2 α , rendering the translation machinery inactive. Viruses have developed strategies for preventing the action of PKR, one of which is the production of small RNAs that inhibit the enzyme. Epstein–Barr virus (EBV) encodes EBER1, a 167 nucleotide non-coding RNA that is constitutively expressed by the EBV-infected cells. EBER1 binds PKR *in vitro* and has been shown to prevent inhibition of translation by PKR *in vitro*. We used affinity cleavage by the EDTA-Fe-modified double-stranded RNA-binding domain (dsRBD) of PKR to show that stem–loop IV (nucleotides 87–123) of EBER1 makes specific contacts with the dsRBD. To further demonstrate the specificity of this interaction, we generated a deletion mutant of EBER1, comprising only stem–loop IV (mEBER1). Cleavage patterns produced on mEBER1 by the bound dsRBD were remarkably similar to those found on full-length EBER1. Using cleavage data from two different dsRBD mutants, we present a model of the interaction of PKR dsRBD and mEBER1.

INTRODUCTION

The protein kinase dependent on RNA (PKR) is an interferon-inducible enzyme that is found in the cytoplasm and is a part of the intracellular anti-viral response (Meurs *et al.*, 1990; Kaufman, 1999; Williams, 1999). RNA duplexes longer than ~24 bp are able to bind and activate PKR, a process that includes PKR dimerization and autophosphorylation (Galabru and Hovanessian, 1987; Patel *et al.*, 1995). Once activated, the enzyme is capable of phosphorylating the α subunit of the translation initiation factor eIF-2, which causes the translation to cease (de Haro *et al.*, 1996). Viruses have developed numerous ways to circumvent the effects of PKR (Clemens *et al.*, 1994; Jagus and Gray, 1994; Gale and Katze, 1998). Adenovirus and Epstein–Barr virus (EBV)

synthesize highly structured RNAs designated VA and EBER, respectively (Kitajewski *et al.*, 1986; Clarke *et al.*, 1990). These RNAs bind PKR and block its activation, allowing continued translation in the cell. In addition to its anti-viral activity, PKR has been shown to be involved in apoptotic pathways (Lee and Esteban, 1994; Der *et al.*, 1997).

Human PKR is 68 kDa, consisting of a 20 kDa N-terminal double-stranded RNA-binding domain (dsRBD) and a C-terminal kinase domain (Meurs *et al.*, 1990). The dsRBD is composed of two copies of the dsRNA-binding motif (dsRBM), an ~70 amino acid motif found in many dsRNA-binding proteins. The mode of dsRBM binding to dsRNA is believed to be largely sequence independent. The solution structure of the 20 kDa PKR dsRBD was determined by NMR spectroscopy and shows that both dsRBMs have the characteristic α – β – β – α fold (Nanduri *et al.*, 1998). A crystal structure of the dsRBM II from *Xenopus laevis* RNA-binding protein A (Xlrpba) bound to dsRNA revealed that the dsRBM spans a major and two flanking minor grooves (~16 bp). Contacts to the grooves are made using three clusters of amino acids, designated regions I, II and III of the dsRBM (Ryter and Schultz, 1998).

EBV is a human B-cell lymphotropic herpesvirus and the causative agent of infectious mononucleosis. The virus has also been associated with several malignant diseases, such as Burkitt's lymphoma and nasopharyngeal carcinoma (Klein, 1989). In these diseases, EBV establishes a persistent infection (latent state) and constitutively expresses several gene products, including EBER1 and EBER2 RNAs (Laing *et al.*, 2001). The physiological function of EBERs is still controversial. One study showed that EBV without the EBER genes was capable of both infecting and transforming primary B lymphocytes (Swaminathan *et al.*, 1991). However, the fact that EBV has retained the EBER genes during the course of evolution is evidence that these RNAs play a role in the life cycle of the virus.

*Corresponding author. Tel: +1 801 585 9719; Fax: +1 801 581 8433; E-mail: beal@chem.utah.edu

EBER1 and EBER2 are 167- and 172-nucleotide-long RNAs with extensive secondary structure (Glickman *et al.*, 1988). Both RNAs are found in the cytoplasm, as well as in the nucleus of the EBV-infected cells (Schwemmler *et al.*, 1992). Data suggest that at least one of the roles of EBERs is to inhibit the activity of PKR. EBERs were found to bind PKR *in vitro* (Sharp *et al.*, 1993). Also, using an *in vitro* reticulocyte lysate system, it was shown that EBER1 prevented inhibition of protein synthesis caused by dsRNA activation of the PKR endogenous to the lysate (Clarke *et al.*, 1990). In addition, EBERs are capable of functionally substituting for VAI RNA in adenovirus-infected cells (Bhat and Thimmappaya, 1985). Yamamoto *et al.* (2000) carried out experiments to establish a connection between EBERs and the role of PKR in apoptosis. The study demonstrated that EBV-negative B-lymphoma cells became resistant to apoptotic stimuli when they expressed EBERs. The authors suggest that this effect arises from the EBERs preventing PKR from inducing apoptosis. However, since the binding site for PKR on the EBERs had not been identified and other host proteins are known to interact with EBERs, it could not be unequivocally established that the interaction with PKR was responsible for this observed effect.

Because the relative abundance of EBER1 is at least 10-fold higher than that of EBER2 *in vivo* (Clarke *et al.*, 1992), our study focused on EBER1. Experiments have shown that PKR and EBER1 interact *in vitro*. However, the molecular details of this complex are unknown. It was previously demonstrated that EBER1 binds the ribosomal protein L22 with the stem-loop III (Toczyski *et al.*, 1994) and the La antigen with the terminal stem and 3' end (Glickman *et al.*, 1988). We wanted to know whether EBER1 used one of these or a different structural element to interact with PKR. However, it was not possible to predict which part of such a complex RNA structure PKR would bind.

In this study, we used three different PKR dsRBD mutants modified with a hydroxyl radical-generating EDTA-Fe group (Spanggard and Beal, 2001). Affinity cleavage on EBER1 stemming from the EDTA-Fe-modified E29C and D38C mutant dsRBDs helped us understand not only the location of the dsRBM I on EBER1, but also its orientation. A mutant in the dsRBM II analogous to the E29 position (Q120C) was employed to attempt to locate the dsRBM II on EBER1. Using affinity cleavage data from EDTA-Fe-modified dsRBD mutants, we were able to identify the EBER1 sequences involved in PKR binding, as well as present a molecular model of the complex formed between EBER1 and dsRBM I of PKR.

RESULTS AND DISCUSSION

Mutant dsRBDs bind EBER1 with affinities similar to wild-type (WT) dsRBD

We performed side-by-side binding assays and found that all EDTA-Fe-modified dsRBD mutants used in this study bind EBER1 with similar affinity to that of the WT dsRBD (Figure 1). As can be seen in Figure 1, WT dsRBD, E29C* and D38C* fully shifted the EBER1 band at 5 μ M protein concentration (lane 5). Q120C* exhibited the same behavior in lane 6, where a 10 μ M concentration was used. We concluded that the mutations and modifications of the dsRBD do not significantly affect the EBER1 binding affinity.

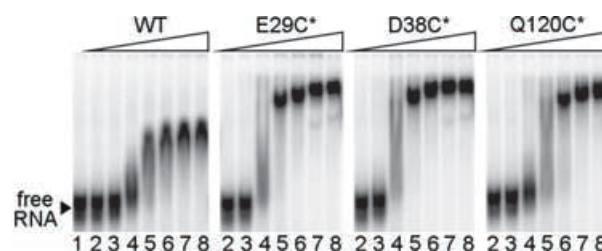


Fig. 1. Gel mobility shift assays for EBER1 binding to WT dsRBD and EDTA-Fe-modified mutants. Lane 1 is a no-protein control, whereas other lanes contain the dsRBD at the following concentrations: lane 2, 0.1 μ M; lane 3, 0.5 μ M; lane 4, 2 μ M; lane 5, 5 μ M; lane 6, 10 μ M; lane 7, 20 μ M; lane 8, 30 μ M.

PKR dsRBD interacts with stem-loop IV of EBER1

Even though PKR-EBER1 binding has been studied previously, the part of the RNA responsible for binding PKR has not been determined. The affinity cleavage of EBER1 by the EDTA-Fe-modified D38C and E29C (D38C* and E29C*, respectively) identified the stem-loop IV of the RNA as the binding site for PKR dsRBD (Figure 2). From these experiments, it seemed that the dsRBM I was binding the stem-loop IV in two different locations: one at the loop end of the stem and the other close to the opposite end. There were no other nucleotides in EBER1 that were cleaved by these two mutant dsRBDs. To understand the dsRBD-EBER1 complex better, we attempted to cleave both 5'- (Figure 2) and 3'-labeled RNA (data not shown) with Q120C*, a residue in dsRBM II of PKR. However, we did not observe any localized cleavage caused by this mutant.

Previous experiments have suggested that the dsRBM II may be an autoinhibitory domain of PKR. This suggests that activating RNAs may differ from inhibiting RNAs in their ability to bind the dsRBM II and relieve the inhibition of the catalytic domain. Using NMR spectroscopy, Qin and co-workers showed that when the dsRBD was added to the PKR kinase domain *in trans*, the dsRBM II made contacts with the catalytic portion of the enzyme (Nanduri *et al.*, 2000). Furthermore, affinity cleavage data from several PKR-RNA complexes support the hypothesis that activating RNAs bind both dsRBMs, whereas inhibiting RNAs can sequester PKR by binding only one dsRBM, leading to an inactive complex (Spanggard *et al.*, 2002). Our findings strengthen this hypothesis by demonstrating that EBER1 only interacts with the dsRBM I, allowing the dsRBM II to inhibit the kinase domain of PKR.

Isolated stem-loop IV of EBER1 is sufficient for dsRBD binding

To confirm that the rest of EBER1 was not critical for binding to PKR dsRBD, we synthesized the isolated stem-loop IV, comprising nucleotides 87–123 (mEBER1; Figure 3). When cleaved with E29C*, the cleavage patterns on this RNA were remarkably similar to those observed on full-length EBER1. Minor differences in the patterns can be attributed to small variations in the conformation of the stem-loop IV, depending on whether its ends are free or fixed by flanking sequences in EBER1. In addition, in an EBER1-dsRBD complex, parts of EBER1 outside the stem-loop IV may be interacting with the

M. Vuyisich, R.J. Spangord & P.A. Beal

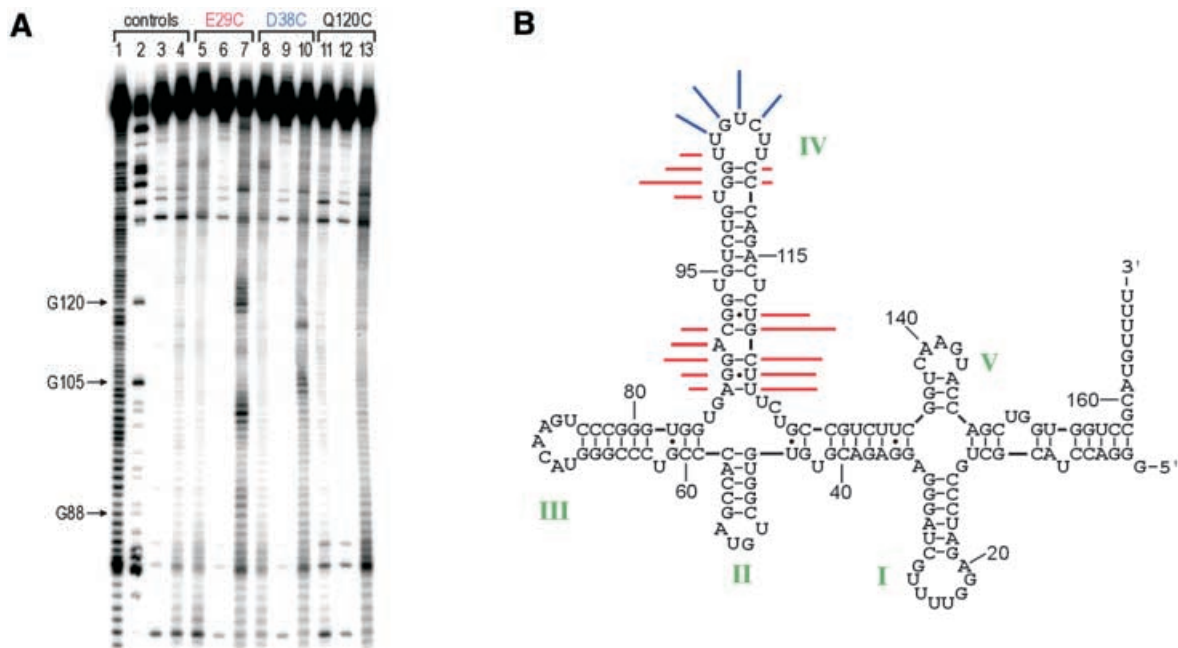


Fig. 2. Affinity cleavage of EBER1 using the EDTA-Fe-modified dsRBD. (A) Six percent gel separating the 5' end-labeled RNA cleavage products. Lane 1, alkaline hydrolysis; lane 2, G lane (RNase T1); lane 3, RNA only; lane 4, RNA + Reagents; lane 5, RNA + E29C^o + Reagents + 4 μM EDTA-Fe; lane 6, RNA + E29C*^o; lane 7, RNA + E29C* + Reagents; lane 8, RNA + D38C^o + Reagents + 4 μM EDTA-Fe; lane 9, RNA + D38C*^o; lane 10, RNA + D38C* + Reagents; lane 11, RNA + Q120C^o + Reagents + 8 μM EDTA-Fe; lane 12, RNA + Q120C*^o; lane 13, RNA + Q120C* + Reagents. (B) Cleavage sites produced by E29C* (red) and D38C* (blue) are mapped onto EBER1 secondary structure, where line lengths indicate relative cleavage efficiencies. Roman numerals in green are used to number the stem-loops on EBER1. The apparent localized cleavage near nucleotide 117 arises from the compression of three bands.

dsRBD non-specifically and influence minor changes in its position.

With D38C*, nucleotides in the single-stranded loop of mEBER1 were cleaved most efficiently. This dsRBD mutant also cleaved these nucleotides in full-length EBER1. Interestingly, a weak cleavage pattern was observed at the ends of mEBER1 with D38C*, which was not detected with the full-length RNA. It is possible that when the dsRBD is bound to the full-length RNA, the D38 residue is directed into a structure where the cleavage is diffused over many nucleotides, thus merging with the background. In the case of mEBER1, however, only the end base pairs are exposed to the modified D38 residue.

Although no localized cleavage was observed with Q120C* on EBER1, weak cleavage is observed with this mutant on mEBER1. This cleavage is diffused over several nucleotides with two enhanced sites (G19–C21 and C30–U31). One possible explanation for mEBER1 cleavage is that dsRBM II non-specifically binds any available RNA surface (by electrostatic interactions). In the case of EBER1, this non-specific binding occurs at different locations in the RNA. Shorter mEBER1, however, provides limited surface area for dsRBM II binding, allowing longer-lived complexes to exist, leading to localized cleavage.

A model of the PKR dsRBM I–mEBER1 complex

Based on the affinity cleavage data, we built a molecular model of the dsRBM I–mEBER1 complex (Figure 4). To explain the cleavage observed at both ends of the RNA, we suggest that dsRBM I has two binding sites on stem-loop IV of EBER1: one at the loop end of the stem (Figure 4A) and the other close to the

opposite end (Figure 4B). Given the two binding sites for dsRBM I on this stem, it is possible that EBER1 is capable of binding two dsRBDs simultaneously. This property could contribute to the potency of this kinase inhibitor because one EBER1 molecule could sequester two molecules of PKR without activating the catalytic domain of the enzyme.

Currently, EBER1 is known to interact with three cellular proteins: the La antigen, the ribosomal L22 protein and PKR. The La antigen binds the terminal stem and the U-rich 3' end of EBER1 (Glickman *et al.*, 1988). The ribosomal protein L22 interacts with the stem-loop III (Toczyski *et al.*, 1994), and we show here that the PKR dsRBD makes contacts with the stem-loop IV of EBER1. Even though the physiological relevance of these interactions is uncertain, it is interesting that three host proteins bind EBER1 at three different locations. This observation raises the possibility that EBER1 is able to simultaneously inhibit two or three cellular targets by employing distinct structural and functional 'domains'. Further studies with mutants of EBER1 with deleted binding sites for its various protein targets should shed light on the purpose of these interactions, as well as reveal which domain is responsible for causing resistance to apoptosis observed when EBERs are expressed in an EBV-negative B-lymphoma cell line.

METHODS

General. Distilled, deionized water was used for all aqueous reactions and dilutions. Biochemical reagents were obtained from Sigma/Aldrich unless otherwise noted. Restriction enzymes and nucleic acid-modifying enzymes were purchased from New England Biolabs. Oligonucleotides were prepared on a Perkin

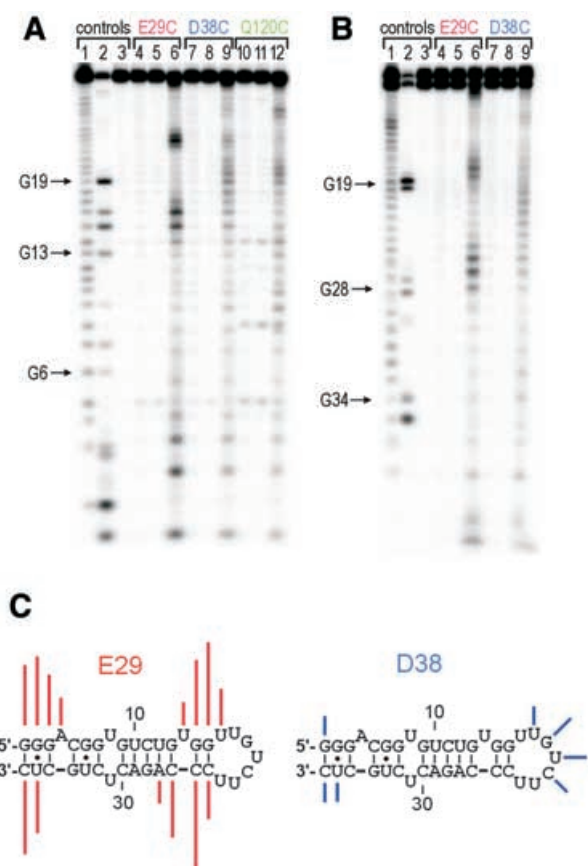


Fig. 3. Affinity cleavage of mEBER1 using EDTA-Fe-modified dsRBD. **(A)** Fifteen percent gel separating the 5' end-labeled RNA cleavage products. Lane 1, alkaline hydrolysis; lane 2, G lane (RNase T1); lane 3, RNA only; lane 4, RNA + E29C^o + Reagents + 16 μM EDTA-Fe; lane 5, RNA + E29C* + Reagents; lane 6, RNA + E29C* + Reagents + 16 μM EDTA-Fe; lane 7, RNA + D38C^o + Reagents + 16 μM EDTA-Fe; lane 8, RNA + D38C* + Reagents; lane 9, RNA + D38C* + Reagents + 16 μM EDTA-Fe; lane 10, RNA + Q120C^o + Reagents + 32 μM EDTA-Fe; lane 11, RNA + Q120C* + Reagents; lane 12, RNA + Q120C* + Reagents. **(B)** Fifteen percent gel separating the 3' end-labeled RNA cleavage products. Lane 1, alkaline hydrolysis; lane 2, G lane (RNase T1); lane 3, RNA only; lane 4, RNA + E29C^o + Reagents + 16 μM EDTA-Fe; lane 5, RNA + E29C* + Reagents; lane 6, RNA + E29C* + Reagents; lane 7, RNA + D38C^o + Reagents + 16 μM EDTA-Fe; lane 8, RNA + D38C* + Reagents; lane 9, RNA + D38C* + Reagents + 16 μM EDTA-Fe; lane 10, RNA + D38C* + Reagents + 16 μM EDTA-Fe; lane 11, RNA + D38C* + Reagents + 16 μM EDTA-Fe; lane 12, RNA + D38C* + Reagents + 16 μM EDTA-Fe. **(C)** Cleavage sites produced by E29C* (red) and D38C* (blue) are mapped onto mEBER1 secondary structure, where line lengths indicate relative cleavage efficiencies. Cleavage efficiencies at nucleotides 36 and 37 for both D38C* and E29C* were determined from the gel in (B). When mEBER1 RNA was 3' end labeled, *n* - 1 product appeared upon storage, producing shadow bands in the G lane.

Elmer/ABI Model 392 DNA/RNA synthesizer with β-cyanoethyl phosphoramidites. 5'-dimethoxytrityl-protected 2'-deoxyadenosine, 2'-deoxyguanosine, 2'-deoxycytidine and thymidine phosphoramidites were purchased from Perkin Elmer/ABI. [γ -³²P]ATP (6000 Ci/mmol) and [³²P]pCp (3000 Ci/mmol) were obtained from DuPont NEN. Storage phosphor autoradiography was carried out using imaging plates purchased from Kodak. A Molecular Dynamics STORM 840 was used to obtain all data from phosphor-imaging plates. Bromoacetamidobenzyl-EDTA-Fe was purchased from Dojindo Laboratories.

Preparation of dsRBD. All proteins used in this study were prepared as described previously (Spangord and Beal, 2001). In this report, PKR dsRBD mutants with a superscripted o denote a

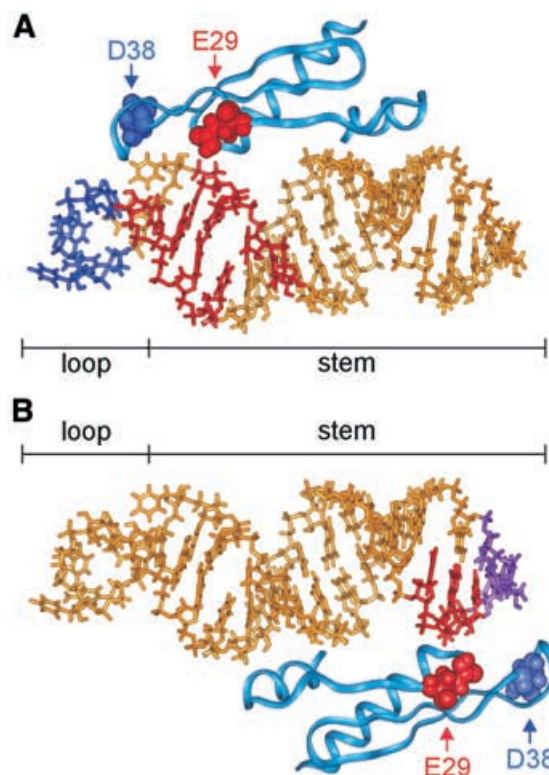


Fig. 4. Models of the two complexes formed between PKR dsRBM I and mEBER1 based on the observed cleavage data. EDTA-Fe-modified amino acid positions with the corresponding cleaved nucleotides are highlighted in color. In **(B)**, the nucleotides cleaved by both E29C* and D38C* are shown in purple.

protein that has not been modified with EDTA-Fe, whereas a superscripted asterisk denotes a modified protein.

Preparation of EBER1. An insert coding for EBER1 was prepared from two ~110 bp DNA oligonucleotides and cloned into pUC-19 vector using a three-piece ligation. The insert consisted of a T7 promoter and EBER1 coding sequence, which ends with a *Dral* restriction site. The sequence of the insert was confirmed by dideoxy DNA sequencing (University of Utah Core Sequencing Facility). An isolated plasmid (pUC-EBER1) was digested with *Dral* and used as a template for run-off transcription by T7 RNA polymerase (Stratagene). The 167-nucleotide-long transcript differs from the WT EBER1 sequence only by having its 5' adenosine replaced by a guanosine. Transcription reactions were resolved on a 10% denaturing polyacrylamide gel, from which EBER1 was extracted. The RNA was then treated with shrimp alkaline phosphatase (SAP) and DNase I, followed by another gel purification. This 5'-dephospho EBER1 was used for both 5' and 3' end labeling.

Preparation of stem-loop IV from EBER1 (mEBER1). mEBER1 was transcribed off a single-stranded DNA template with duplex DNA present only in the T7 promoter region (Milligan and Uhlenbeck, 1989). Our 37 nucleotide mEBER1 differs from the WT sequence in that the closing base pair of the stem is a G-C instead of an A-U. After the transcription reaction and gel purification, mEBER1 was SAP and DNase I treated, followed by another gel purification. This RNA was used for both 5' and 3' end labeling.

M. Vuyisich, R.J. Spangord & P.A. Beal

EBER1–dsRBD binding assays. We utilized gel mobility shift assays for estimating binding affinities. These were carried out by incubating 1 nM EBER1 with increasing amounts of each protein in affinity cleavage buffer for 7 min, followed by the addition of glycerol and loading on a running 10% (79:1) gel. Bands were visualized using autoradiography.

Affinity cleavage experiments. These experiments were performed as described previously (Spangord and Beal, 2001). In brief, small amounts of end-labeled RNA (<5 nM), tRNA^{Phe} from baker's yeast (30 µg/ml) and EDTA-Fe-modified dsRBD were incubated for 7 min in a final volume of 16 µl of affinity cleavage buffer (25 mM Tris-HCl, 10 mM NaCl pH 7). For cleaving EBER1, 4 µM E29C and D38C, and 8 µM Q120C were used, whereas 16 µM E29C and D38C, and 32 µM Q120C were used for cleaving mEBER1. Hydrogen peroxide at a final concentration of 0.001% and ascorbic acid at a final concentration of 5 mM (called 'Reagents') were added at 2 µl each. After 5 min, the reactions were quenched with 20 µl of formamide loading buffer (96% formamide, 0.2× TBE) that was heated to 95°C. The reactions were then placed in a 95°C bath for 3 min and 4 µl of each were loaded onto a denaturing polyacrylamide gel. EBER1 reactions were loaded onto a 6% gel, whereas mEBER reactions were resolved on a 15% gel. Gels were dried and visualized using imaging plates. To quantify the RNA cleavage at each nucleotide, the intensity of a band (in pixels) in the lane with unmodified protein plus reagents and free EDTA-Fe was subtracted from the intensity of the band in the lane with modified protein plus reagents. The amount of cleavage at each nucleotide is displayed as a line of length proportional to the cleavage intensity. Only those sites where the cleavage was ≥20 times over the background are plotted.

Molecular modeling. Molecular modeling was performed on a Silicon Graphics O₂ work station running Insight II (Biosym). All minimizations were performed using Discover 3 module with Amber forcefield. First, the stem of mEBER1 was built and minimized. The loop nucleotides were then appended and minimized. The PKR dsRBM I was generated using the crystal structure coordinates reported for the Xlrbpa dsRBM II (Ryter and Schultz, 1998). The E29 amino acid position of the PKR dsRBM I was mapped onto the ribbon structure of the Xlrbpa dsRBM II using the analogous V133 amino acid position and the homology modeling module in Insight II (Fierro-Monti and Mathews, 2000). The D38 amino acid position of the PKR dsRBM I was mapped using the analogous K142 amino acid position of the Xlrbpa dsRBM II. Docking of the PKR dsRBM I was carried manually in Insight II, maintaining the locations of the three regions of RNA contact observed in the Xlrbpa dsRBM II–dsRNA structure and guided by the cleavage data obtained in this work.

ACKNOWLEDGEMENTS

The authors would like to acknowledge a grant from the National Institutes of Health (GM57214) for funding this research.

REFERENCES

Bhat, R.A. and Thimmappaya, B. (1985) Construction and analysis of additional adenovirus substitution mutants confirm the complementation of VAI RNA function by two small RNAs encoded by Epstein–Barr virus. *J. Virol.*, **56**, 750–756.

Clarke, P.A., Sharp, N.A. and Clemens, M.J. (1990) Translational control by the Epstein–Barr virus small RNA EBER-1. Reversal of the double-stranded RNA-induced inhibition of protein synthesis in reticulocyte lysates. *Eur. J. Biochem.*, **193**, 635–641.

Clarke, P.A., Sharp, N.A. and Clemens, M.J. (1992) Expression of genes for the Epstein–Barr virus small RNAs EBER-1 and EBER-2 in Daudi Burkitt's lymphoma cells: effects of interferon treatment. *J. Gen. Virol.*, **73**, 3169–3175.

Clemens, M.J., Laing, K.G., Jeffrey, I.W., Schofield, A., Sharp, T.V., Elia, A., Matys, V., James, M.C. and Tilleray, V.J. (1994) Regulation of the interferon-inducible eIF2 α protein kinase by small RNAs. *Biochimie*, **76**, 770–778.

de Haro, C., Mendez, R. and Santoyo, J. (1996) The eIF-2 α kinases and the control of protein synthesis. *FASEB J.*, **10**, 1378–1387.

Der, S.D., Yang, Y., Weissmann, C. and Williams, B.R.G. (1997) A double-stranded RNA-activated protein kinase-dependent pathway mediating stress-induced apoptosis. *Proc. Natl Acad. Sci. USA*, **94**, 3279–3283.

Fierro-Monti, I. and Mathews, M.B. (2000) Proteins binding to duplexed RNA: one motif, multiple functions. *Trends Biochem. Sci.*, **25**, 241–246.

Galabru, J. and Hovanessian, A. (1987) Autophosphorylation of the protein kinase dependent on double-stranded RNA. *J. Biol. Chem.*, **262**, 15538–15544.

Gale, M.J. and Katze, M.G. (1998) Molecular mechanisms of interferon resistance mediated by viral-directed inhibition of PKR, the interferon-induced protein kinase. *Pharmacol. Ther.*, **78**, 29–46.

Glickman, J.N., Howe, G. and Steitz, J.A. (1988) Structural analyses of EBER1 and EBER2 ribonucleoprotein particles present in Epstein–Barr virus-infected cells. *J. Virol.*, **62**, 902–911.

Jagus, R. and Gray, M.M. (1994) Proteins that interact with PKR. *Biochimie*, **76**, 779–791.

Kaufman, R.J. (1999) Double-stranded RNA-activated protein kinase mediates virus-induced apoptosis: a new role for an old factor. *Proc. Natl Acad. Sci. USA*, **96**, 11693–11695.

Kitajewski, J., Schneider, R.J., Safer, B., Munemitsu, S.M., Samuel, C.E., Thimmappaya, B. and Shenk, T. (1986) Adenovirus VAI RNA antagonizes the antiviral action of interferon by preventing activation of the interferon-induced eIF-2 α kinase. *Cell*, **45**, 195–200.

Klein, G. (1989) Viral latency and transformation: the strategy of Epstein–Barr virus. *Cell*, **58**, 5–8.

Laing, K.G., Matys, V. and Clemens, M.J. (2001) Analysis of the expression and function of the EBV-encoded small RNAs, the EBERs, in heterologous cells. *Methods Mol. Biol.*, **174**, 45–66.

Lee, S.B. and Esteban, M. (1994) The interferon-induced double-stranded RNA-activated protein kinase induces apoptosis. *Virology*, **199**, 491–496.

Meurs, E., Chong, K., Galabru, J., Thomas, N.S.B., Kerr, I.M., Williams, B.R.G. and Hovanessian, A. (1990) Molecular cloning and characterization of the human double-stranded RNA-activated protein kinase induced by interferon. *Cell*, **62**, 379–390.

Milligan, J.F. and Uhlenbeck, O.C. (1989) Synthesis of small RNAs using T7 RNA polymerase. *Methods Enzymol.*, **180**, 51–62.

Nanduri, S., Carpick, B.W., Yang, Y., Williams, B.R.G. and Qin, J. (1998) Structure of the double-stranded RNA-binding domain of the protein kinase PKR reveals the molecular basis of its dsRNA-mediated activation. *EMBO J.*, **17**, 5458–5465.

Nanduri, S., Rahman, F., Williams, B.R.G. and Qin, J. (2000) A dynamically tuned double-stranded RNA binding mechanism for the activation of antiviral kinase PKR. *EMBO J.*, **19**, 5567–5574.

Patel, R.C., Stanton, P., McMillan, N.M.J., Williams, B.R.G. and Sen, G.C. (1995) The interferon-inducible double-stranded RNA-activated protein kinase self-associates *in vitro* and *in vivo*. *Proc. Natl Acad. Sci. USA*, **92**, 8283–8287.

Ryter, J.M. and Schultz, S.C. (1998) Molecular basis of double-stranded RNA–protein interactions: structure of a dsRNA-binding domain complexed with dsRNA. *EMBO J.*, **17**, 7505–7513.

Schwemmler, M., Clemens, M.J., Hilse, K., Pfeifer, K., Troster, H., Muller, W.E.G. and Bachmann, M. (1992) Localization of Epstein–Barr virus-encoded RNAs EBER-1 and EBER-2 in interphase and mitotic Burkitt lymphoma cells. *Proc. Natl Acad. Sci. USA*, **89**, 10292–10296.

- Sharp, T.V., Schwemmler, M., Jeffrey, I., Laing, K., Mellor, H., Proud, C.G., Hilse, K. and Clemens, M.J. (1993) Comparative analysis of the regulation of the interferon-inducible protein kinase PKR by Epstein-Barr virus RNAs EBER-1 and EBER-2 and adenovirus VA₁ RNA. *Nucleic Acids Res.*, **21**, 4483–4490.
- Spangord, R.J. and Beal, P.A. (2001) Selective binding by the RNA-binding domain of PKR revealed by affinity cleavage. *Biochemistry*, **40**, 4272–4280.
- Spangord, R.J., Vuyisich, M. and Beal, P.A. (2002) Identification of binding sites for both dsRBMs of PKR on kinase-activating and kinase-inhibiting RNA ligands. *Biochemistry*, **41**, 4511–4520.
- Swaminathan, S., Tomkinson, B. and Kieff, E. (1991) Recombinant Epstein-Barr virus with small RNA (EBER) genes deleted transforms lymphocytes and replicates *in vitro*. *Proc. Natl Acad. Sci. USA*, **88**, 1546–1550.
- Toczyski, D.P., Matera, A.G., Ward, D.C. and Steitz, J.A. (1994) The Epstein-Barr virus (EBV) small RNA EBER1 binds and relocalizes ribosomal protein L22 in EBV-infected human B lymphocytes. *Proc. Natl Acad. Sci. USA*, **91**, 3463–3467.
- Williams, B.R.G. (1999) PKR; a sentinel kinase for cellular stress. *Oncogene*, **18**, 6112–6120.
- Yamamoto, N., Tokizawa, T., Iwanaga, Y., Shimizu, N. and Yamamoto, N. (2000) Malignant transformation of B lymphoma cell line BJAB by Epstein-Barr virus-encoded small RNAs. *FEBS Lett.*, **484**, 153–158.

DOI: 10.1093/embo-reports/kvf137